A Pragmatic Approach to Exploiting Full Force Capacity for Serial Redundant Manipulators

David Busson and Richard Béarée

***Abstract*—Considering a set of robotic tasks which involve physical interaction with the environment, the theoretical knowledge of the full force capacity of the manipulator is a key factor in the design or development of an efficient and economically attractive solution. Carrying its own weight while countering forces may be too much for a robot in certain configurations. Kinematic redundancy with regard to a task allows a robot to perform it in a continuous space of articular configurations; space in which the payload of the robot may vary dramatically. It may be impossible to withstand a physical interaction in some configurations, while it may be easily sustainable in others that bring the end-effector to the same location. This becomes obviously more prevalent for a limited payload robot. This letter describes a framework for these kind of operations, in which kinematic redundancy is used to explore the full extent of a force capacity for a given manipulator and task (in this letter, the terms "force" and "wrench" may interchangeably refer to two-, three-, or six-dimensional forces depending on the dimension of the problem and on whether they may or may not include components of translational forces and/or moments. Their dimensional definition will be explicitly given whenever specifically needed). A pragmatic force capacity index (FCI) is proposed. The FCI offers a sound basis for redundancy resolution via optimization or complete redundancy exploration, and may provide good hints for end-effector design. A practical use case involving 7-DOFs KUKA LBR iiwa was used to demonstrate the relevance of the proposed method.**

***Index Terms*—Industrial robots, redundant robots, kinematics.**

I. Introduction

RECENT developments in lightweight robotics put versatility on center stage. This versatility is however often hampered by their limited force capacity. This is still an obstacle to have these manipulators populate a larger portion of the industrial robotic scene. The idea behind this letter comes from our participation to the Airbus Shopfloor Challenge taking place at ICRA 2016 Stockholm (see Fig. 1), where a frustrating need for a redundancy exploitation to the benefit of force capacity emerged. Years of study on the subject of poly-articulated mechanisms have achieved to show us that the force capacity of a robot strongly depends on its articular configuration [1]–[6]. We propose in this article to exploit these variations to the manipulators' advantage.

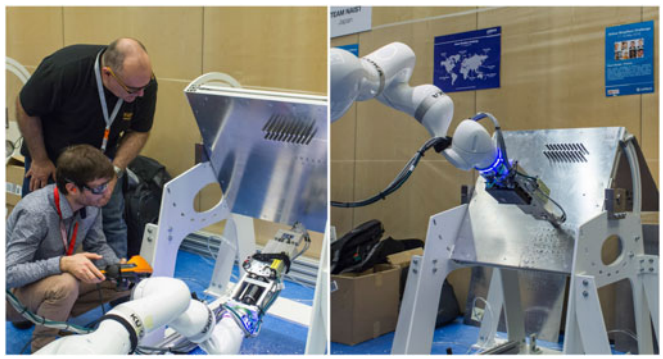

Fig. 1. 7-joints LBR iiwa during the Airbus Shopfloor Challenge, ICRA 2016, Stockholm.

Yoshikawa introduced the concept of force manipulability ellipsoids [1]. These ellipsoids are ways of representing, in a given articular configuration, the force transmission efficiency of serials manipulators. The force ellipsoid is defined as the forces created by the set of all possible torque vectors whose norm is equal to one, when the manipulator is in a given posture. This sphere of articular torques is mapped, thanks to the Jacobian matrix of the manipulator, into Cartesian space to form an ellipsoid of Cartesian forces. Yoshikawa also designed the concept of dynamic manipulability ellipsoids [7], which accounts for the efficiency of a manipulator to produce accelerations of its end-effector. This concept was refined to better take into account the effect of gravity [8] and Chiacchio and Concilio later formulated a version of this ellipsoid for redundant manipulators and non-redundant manipulator in singular configurations [2], [9]. On the downside, ellipsoids only provide an approximate description of the performance of a manipulator [10], for they are derived from a l_2 norm rather that from a l_∞ norm, which prevents them from transforming the exact joint constraints into task space [11].

The force polytopes [3] are another well known tool for describing dexterity. Force polytopes have the ability to accurately describe maximum achievable force capacity of manipulators, because they derive from a l_∞ norm. A force polytope is

Manuscript received September 8, 2017; accepted December 26, 2017. Date of publication January 12, 2018; date of current version February 1, 2018. This letter was recommended for publication by Associate Editor Y. Choi and Editor W. K. Chung upon evaluation of the reviewers' comments. This work was supported by Kuka Systems Aerospace France. *(Corresponding author: David Busson.)*

The authors are with the Laboratoire des Sciences de l'Information et des Systèmes (LSIS UMR C.N.R.S. 7296), Arts et Métiers ParisTech, Lille 59046, France (e-mail: david.busson@ensam.eu; richard.bearee@ensam.eu).

This letter has supplementary downloadable material available at http://ieeexplore.ieee.org, provided by the authors. The Supplementary Materials contain a video showing the comparison of the force capacities of a robot when its configurations are optimized with the force capacity index (FCI) and when they are not for several end-effector designs. This material is 5.93 MB in size.

Digital Object Identifier 10.1109/LRA.2018.2792541

TABLE I
QUALITATIVE COMPARATIVE STUDY OF DIFFERENT POSTURE-DEPENDENT TOOLS USED FOR WRENCH PRODUCTION PERFORMANCE EVALUATION OF SERIAL REDUNDANT MANIPULATORS

	Force Polytopes	Force Ellipsoids	Manipulability index	DCE Framework	FCI
Requires Gen. Inv. or SVD	Yes	Yes	Yes	No	No
Output type	$2 \times$ 3D polytope	$2 \times$ 3D ellipsoid	Scalar	Accumulated N-D ellipsoids	Scalar
Range of study	All Cartesian directions	All Cartesian directions	All Cartesian directions	All Cartesian directions	Focused on a single wrench
Can estimate specific wrench production performance	Yes, for pure force/moment	Yes, for pure force/moment	No	Yes, but at a great cost	Yes
Combines forces/moments in a physically meaningfull manner	No	No	No	Yes	Yes
Independence of scale and unit	No	No	No	Yes	Yes
Handles well singular config. Scales well with #DOFs	No	No	No	Yes	Yes
Analytical expression exists	No	No	No	Yes	Yes

constructed by mapping the exact joint torque constraints, depicted as a convex polytope in articular space, into Cartesian force space, to form a convex polytope. The force polytope provides the exact Cartesian force capability bounds of the robot in all possible Cartesian forces directions for one given posture. They share with ellipsoids problems of homogeneity that arise when using euclidean metrics mixing angular and translational components, and problems of dependency to scale and units [9]. In the redundant or singular case, the computation of polytopes and ellipsoids requires a generalised inversion or Singular Value Decomposition (SVD) of the Jacobian matrix, as well as a projection on the range space of J^T [2], to remain compatible with the static constraints that were outlined in [12].

Later on, Bolwing and Khatib developped the dynamic capability equations (DCE) [4]. This tool expresses the translational and orientational components of Cartesian speed, acceleration, force capacities altogether in joint torque space and makes these immediately comparable in terms of their torque contribution. To do so, spheres of minimal Cartesian speed, acceleration and forces are mapped into joint torque space thanks to the named equation and their corresponding joint torque ellipsoids are accumulated, centering one ellipsoid after the other on the surface of the previous one. This accumulation has to be contained within the joint torque polytope for the manipulator to be able to achieve the minimal performance in terms of the Cartesian quantity in or about any direction. The strengths of this tool are its ability to unify velocity, acceleration and force analysis, while dealing consistently with translations and rotations together.

The methodology proposed in this letter aims at accurately characterising a specific wrench capacity on the full extent of the redundancy space of serial redundant robots to choose a suitable configuration for a given task. The incentive behind this focus on a specific static wrench capacity is that many industrial operations involve specific wrench sustainment and fixed end-effector location. Hence, choosing a suitable destination for this job is very important. Another incentive lives in the need for simplicity and industrial usability of a force capacity criteria. The placement of the base of non-redundant robots and the offline planning (OLP) of redundant robots are often made empirically and without measurable exploitation of their potential benefits, despite the existence of very interesting and global tools, like the ones described before.

The force capacity index (FCI) developed herein is a real-valued index, that exists for an input configuration and an input wrench. This index gives a succinct and quick estimation of the maximum intensity, i.e., the multiplier of the input wrench, that wouldn't saturate any actuator of a manipulator, while the latter is already sustaining its own weight.

II. COMPARISON WITH TRADITIONAL TOOLS

A comparative study of the FCI with traditional force performance evaluation tools is presented in Table I. The ongoing paragraph will complement this table, providing relevant details about each tool, and detailing how and under which assumptions a result equivalent to the FCI output could be obtained from this list of tools. The use of force polytopes would not suit this particular purpose in most cases, as general wrenches mix forces and moments, which can't be meaningfully combined with this tool. For pure force/moment wrenches however, one could try to look at the intersection of the inquired wrench direction (straight line in the relevant Cartesian space) with the surface of the force polytope, which would provide a result equivalent to the FCI's. Force ellipsoids share the same problem of being unable to meaningfully combine forces and moments. Besides, ellipsoids account for force production *efficiency*, not *capacity* (*efficiency* at producing a wrench may be high even though a robot joint is close to a torque limit, thus limiting the robot wrench production *capacity*). Regardless, specific wrench production *efficiency* could be computed for pure force/moment wrenches expressing these wrenches into the singular vectors decomposition associated with the configuration of the system and weighting accordingly with the associated singular values. The manipulability index is encompassing all Cartesian force production *efficiencies* into one single scalar and thus doesn't allow inquiry about a specific wrench production *efficiency*, let alone *capacity*. Using the DCE framework for a specific wrench capacity analysis would

be irrelevantly-computationally expensive. It would require accumulating, within the torque vector space of the manipulator, an ellipsoid corresponding to a pure force wrench that has the same norm as the one coming from the specific wrench with ellipsoids corresponding to a pure moment wrench that has the same norm as the one coming from the specific wrench. Then, it would require scaling up these ellipsoids until the specific wrench lay on the surface of the robot torque polytope. This final scaling factor would then be equivalent to the FCI output. This comparative study clearly highlights the need for such an index.

The methodology proposed in this letter shares with the DCE's its ability to mix Cartesian translational and rotational forces in a physically meaningful manner, and dealing with the problems of dependency on scale and units by focusing on geometric computations in joint torque space. Just like force ellispoids and polytopes, the DCE gives global insights of the force performances of a manipulator, in and about any direction of the Cartesian space. This particular feature is desirable for robot design purpose, or for reactive control applications, where unforeseen physical interactions or reactions may have to be dealt with. This, however, does not count among the explicit focuses of our framework. On the bright side, the FCI behaves very well with high-number-of-DOFs-manipulators, doesn't suffer from singularities, doesn't involve costly computations (such as generalised inversion or SVD), and most importantly has a straightforward formulation and interpretation. These features make it very suitable for redundancy resolution schemes, for easy implementation in autonomous and/or offline programming of redundant robots, in the mechanical design of end-effectors, and possibly in control schemes, although adjustments would have to be done in the latter case to account for dynamic effects. Control schemes won't be exemplified in this letter, which aims at introducing the FCI and apply its use to quasi-static applications.

III. Proposed Methodology

A. Preliminary Remarks on the Redundancy Spaces

The question of exploring the full extent of the redundancy space is no easy job. This space may be partially explored by sampling joint positions in the vicinity of the previous samples thanks to the null space of the Jacobian, but beside the obvious numerical biases, one cannot guarantee to have explored all this space efficiently using this method, especially if it has more than one dimension. A redundancy space, i.e., a space parameterised by well chosen, higher level parameters, is designed to represent the full extent of the self-motion space of the robot performing its task. Changing the position in redundancy space will change the articular configuration of the system without modifying the end-effector task. Kinematic redundancies derive from two main tangled sources, one of them is the release of constraints defining a geometric task, the other is the addition of joints to a well-studied kinematic chain. Without being a rule of thumb, the authors believe that the parameterisation of the redundancy space can often take inspiration from which geometric constraints were freed up, and which internal/external motion were added by "extra" joints in a kinematic chain. A necessary property of this parameterised redundancy space is that picking an *admissible redundancy space position-admissible task* couple leads to a unique set of $k \in \mathbb{N}^{+*}$ articular solutions[1] (when out of singularities). In other words, an inverse geometry step is required to get the lower level inputs that are the joint positions of the manipulator. This parameterisation is convenient here because it allows us to illustrate the variations of the wrench capacity index over the entire redundancy space, and to perform optimisations within it. However, the characterisation of a redundancy space is not strictly needed to compute the value of the wrench capacity index, which only depends on the articular configuration of the manipulator.

An n-DOFs manipulator used for a task $\vec{t}$ of dimension $m < n$ is kinematically redundant. The dimension of the Jacobian null space will be equal to $r = n - m$ in non-singular configurations. r is the number of redundancy parameters that will be used to parameterise the self-motion (or redundancy space) of the robot. Let $\vec{\alpha} = [\,\alpha_1 \quad ... \quad \alpha_r\,]^T$ be the r-dimensional redundancy space position of the manipulator, each α_i being a redundancy parameter. Setting the redundancy space position allows for an unambiguous input formulation of the inverse geometry problem by reducing the number of unknowns of this problem to m in a system of m equations, and provides a finite set of solutions to the inverse geometry problem of the redundant manipulator. A set of articular solutions may be rigorously computed thanks to an *admissible redundancy space position-admissible task* input couple $(\vec{\alpha}, \vec{t})$. Thanks to this formulation, the FCI may be rigorously assessed over the entire redundancy space of the manipulator.

B. The Force Capacity Index λ_{sat}

In the n-dimensional affine space of an n-DOFs manipulator joint torques, let us define the joint torque polytope (see Fig. 2) for a 3-DOFs manipulator) as the convex n-dimensional polyhedron described by the bounding inequalities: $\forall i \in [\![1, n]\!], \tau_{i,l} \leqslant \tau_i \leqslant \tau_{i,u}$, which expresses the fact that the torque of joint i, τ_i, lies within the torque lower bound $\tau_{i,l}$ and the torque upper bound $\tau_{i,u}$ segment.

Let $\vec{f}$ be the wrench, expressed at the TCP,[2] that the manipulator has to sustain at minimum and let $\vec{q}$ be the articular configuration in which to compute the wrench capacity. The gravity torque vector $\vec{\tau}_{\vec{g}}(\vec{q})$, i.e., the vector containing the torque that each actuator of the manipulator will have to produce to counter the effect of weight only, can then be computed thanks to the mass data of the manipulator. Then, the torque vector $\vec{\tau}_{\lambda\vec{f}}$, needed to sustain a lone spatial force $\lambda\vec{f}, \lambda \in \mathbb{R}^+$ in the configuration $\vec{q}$ can be computed thanks to the kinetostatic equation $\vec{\tau}_{\lambda\vec{f}} = \lambda J(\vec{q})^T \vec{f} = \lambda\vec{\tau}_{\vec{f}}$. We will refer to λ as the intensity of the spatial force. During the operation, both $\vec{\tau}_{\vec{g}}$ and $\vec{\tau}_{\lambda\vec{f}}$, with $\lambda = 1$,

[1]The existence of this set of k solutions comes from the periodicity of the trigonometric functions used in the geometric model and is unrelated to kinematic redundancy, as it does not increase the dimension of the redundancy space, but rather multiplies the number of solutions by k.

[2]The TCP, or Tool Center Point, refers to a frame, which is statically attached to the extremal link of the manipulator. This frame is generally placed and oriented at an operating location of the end-effector.

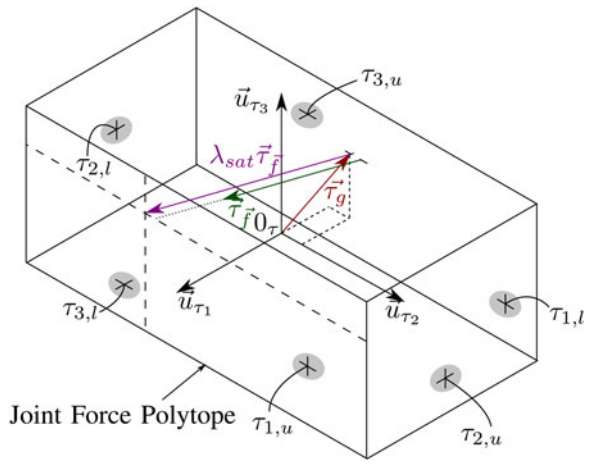

Fig. 2. Joint force polytope for a 3-DOFs manipulator with torque limits $\tau_{i,l}$ and $\tau_{i,u}$ for $i \in [\![1,3]\!]$.

have to be produced at the same time, and we want to know the maximum intensity of the wrench that can be sustained by the manipulator. Determining the wrench capacity comes down to computing the intensity $\lambda_{sat}(\vec{q})$ multiplying the wrench $\vec{f}$ below which no actuator saturates, and from which at least one actuator saturates. This geometrically translates into finding λ_{sat} so that $\vec{\tau}(\vec{q}) = \vec{\tau}_{\vec{g}}(\vec{q}) + \lambda_{sat}\vec{\tau}_{\vec{f}}$ lies on the surface of the joint torque polytope, as can be seen on Fig. 2. Practically, it is therefore interesting to look into the saturating intensity of each actuator, i.e., the minimal intensity $\lambda_i(\vec{q}) \geqslant 0, i \in [\![1,n]\!]$ of the wrench $\vec{f}$ that would overwhelm actuator i, without consideration for the other actuators. This intensity of the wrench produces a torque $\tau_i(\vec{q})$ at actuator i either equal to $\tau_{i,l}$ or to $\tau_{i,u}$. The minimum of the n saturating intensities exactly corresponds to $\lambda_{sat}(\vec{q})$.

$$\forall i \in [\![1,n]\!], \lambda_i = \begin{cases} \frac{\tau_{u,i} - \tau_{\vec{g},i}}{\tau_{\vec{f},i}} & \text{, if } \tau_{\vec{f},i} > 0 \\ \frac{\tau_{l,i} - \tau_{\vec{g},i}}{\tau_{\vec{f},i}} & \text{, if } \tau_{\vec{f},i} < 0 \\ \infty & \text{, if } \tau_{\vec{f},i} = 0 \end{cases}$$

$$\lambda_{sat} = \min((\lambda_i)_{i \in [\![1,n]\!]})$$

C. A Simple Example : 3-DOFs Planar Robot for 2-D Positioning Task, and 2-D Wrench

Let us consider the planar manipulator with three serial revolute joints depicted (for three different configurations) in Fig. 3 for the 2-dimensional planar positioning task while the robot is applying a linear 2-dimensional force $\vec{f}$ at its TCP. The robot is kinematically redundant of order one for the positioning task and therefore has a one dimensional space of articular configurations that allows for the position of its TCP to match the task requirements. The initial step is to find an intuitive parameterisation of the redundancy space. In our situation, a solution could be to take the third joint coordinate of the manipulator, which is, according to the formulation of [13], a monotonic type joint. Indeed, regardless of the goal position occupied by the TCP, fixing the value of this joint angle enables to provide at most one finite set of solutions to the inverse geometric model. An-

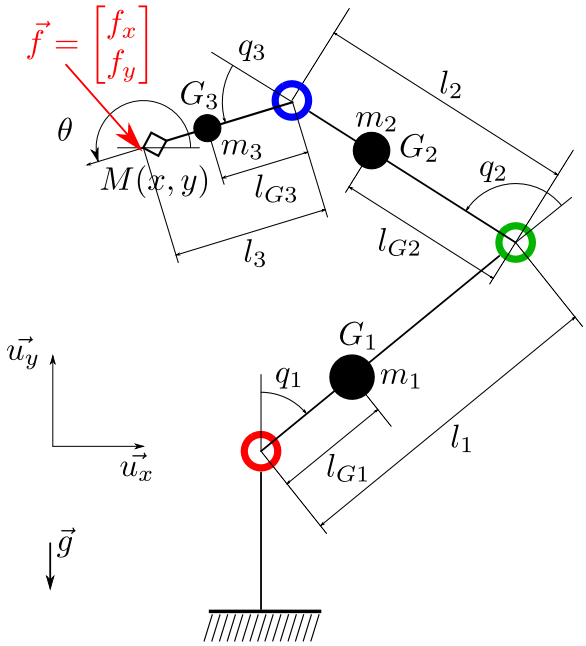

Fig. 3. 3-DOFs planar manipulator settings : $l_1 = .7$ m, $l_2 = .6$ m, $l_3 = .4$ m, $m_1 = 1.5$ kg, $m_2 = 1$ kg, $m_3 = 0.5$ kg, $l_{G1} = 0.5\,l_1$, $l_{G2} = 0.5\,l_2$, $l_{G3} = 0.66\,l_3$, $\tau_{1,u} = -\tau_{1,l} = 20$ Nm, $\tau_{2,u} = -\tau_{2,l} = 9$ Nm, $\tau_{3,u} = -\tau_{3,l} = 6$ Nm. *Note:* Two sets of solutions exist for this planar arm as link 1 and link 2 may also be symmetrically placed on the other side of the joint 1-joint 3 axis. However, only one of these sets will be explored, for the sake of brevity.

other solution for parameterising the redundancy space of the problem is to use the angle θ which corresponds to the angle between the horizontal and the pointing direction of the TCP. Both parameterisations would work, but we will favour the latter (i.e., $\vec{\alpha} = \theta$), because a closed-form expression for the inverse geometry problem is more trivially found this way.

Fig. 4 is a representation of the saturating intensity of the 3 actuators of the manipulator over a significant sampling of $\vec{\alpha} = \theta \in [-\pi, \pi]$. For each sampled θ, the value of λ_{sat} is the minimum value of the saturating intensities λ_1, λ_2 and λ_3. The wrench capacity is shown to greatly depend on the value of the redundancy parameter θ. In this simulated example, λ_{sat} varies everywhere between 0.43 and 1.50. The wrench $\vec{f}$ is not feasible when $\lambda_{sat} < 1$. Drawing a horizontal line at this $\lambda_{sat} = 1$ highlights the admissible ranges of θ for the current task and spatial force, which leaves room for further improvements from a redundancy resolution perspective. In the example, we can see that two spans of values for θ are available for the manipulator to sustain the wrench $\vec{f}$ with an intensity $\lambda_{sat} \geqslant 1$.

Links length and mass, positions of centres of gravity and TCPs, as well as torques limits also have a strong and varying influence on the shape of the saturating intensities. The FCI Can also be an interesting criterion to use during robot or end-effector mechanical design, as is exemplified at the end of the letter.

IV. Application of the Method

Let us apply this method on an existing robot, the KUKA LBR iiwa, for drilling operations. This robot is a 7-DOFs collaborative manipulator with rather limited torque. The

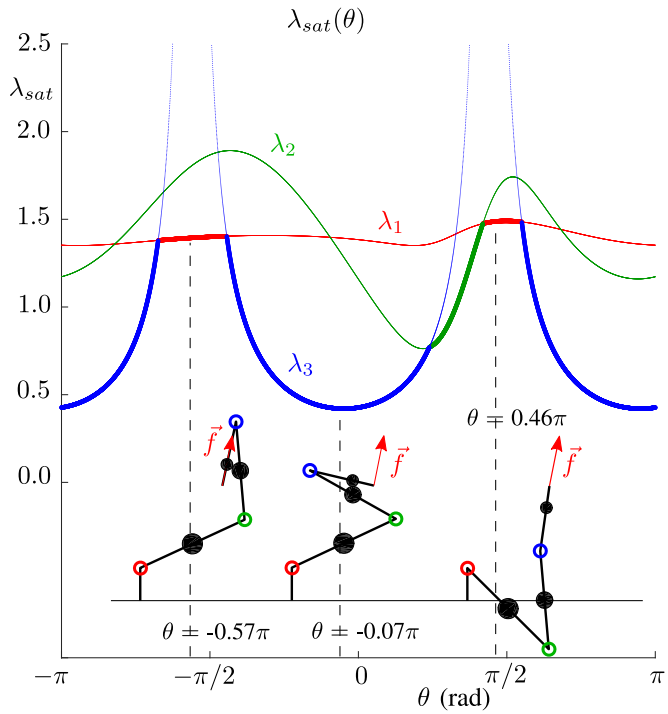

Fig. 4. Joint saturating intensities λ_1, λ_2 and λ_3 (thin lines) and saturating intensity λ_{sat} (thick line) of the 3-DOFs planar robot described in Fig. 3 for $\theta \in [-\pi, \pi]$. Task destination is $M(0.5\text{ (m)}, 0.5\text{ (m)})$ and output force is $\vec{f} = [5.5\text{ (N)}, 27.5\text{ (N)}]^T$ (everything is expressed in the origin reference frame). Some enlightening postures of this manipulator are shown below the curves.

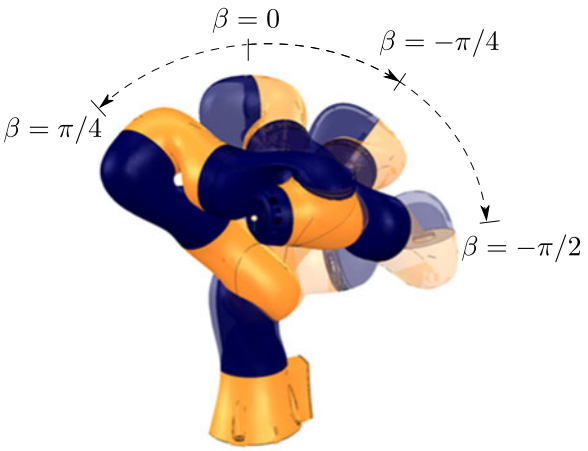

Fig. 5. self-motion of the KUKA LBR iiwa 14 R820 for the traditional 6 DOFS task.

self-motion of this type of manipulator for a fully-constrained task[3] can be parameterized by the "swivel angle" [14] (see Fig. 5), which is based on an angular parameterization of the circular motion of the elbow during the internal-motion of this SRS-anthropomorphic arm. This parameterization directly inherits from the formulations of [15] and [16]. The drilling task is a fully constrained task with a free rotation about the drill axis. Therefore, the drilling task only constrains five DOFs, which leaves us with a 2-redundant-DOFs manipulator. In these condition, we trivially choose to take the rotation about the drill (denoted a_{tcp}) and the swivel angle (denoted β) as parameters for the redundancy parameterization of our problem : $\vec{\alpha} = (\alpha_1, \alpha_2) = (a_{tcp}, \beta)$.

Fig. 6 shows the output of the force capacity evolution over a meaningful sampling of this 2-dimensional redundancy space. In this simulation, λ_{sat} has very sharp variations, with a potential gain that approximates $+290\%$ in the force capacity index. The robot postures associated to three relevant positions in redundancy space are also displayed to give further insight on how the redundancy position influences the general posture of the manipulator while complying with the task, and what makes the robot strong against the spatial force depicted by the red arrow. An intuitive result is that the robot seems stronger when its weakest joints are lightly solicited (in the LBR iiwa, the torque limits range from ± 320 Nm for the first two base joints to ± 40 Nm for the last two joints); e.g., only when joint 6 aligns its rotation axis with the direction of the force does the robot get sharply stronger.[4] On the other hand, joint 6 seems to be highly solicited, with its axis nearly orthogonal to the force direction, in the weaker posture shown in the bottom right of Fig. 6.

A practical use case which consists in drilling a set of y-direction-aligned holes from under a surface with a LBR iiwa (14 kg payload) was simulated and experimentally tested to illustrate a way the FCI could be use for discrete path planning and end-effector mechanical design purposes. Let us suppose that the unfinished design of the end-effector leaves us with two degrees of freedom on the position and orientation of the drill, as illustrated on Fig. 7. The drill rotation and feed motions are exercised by internal mechanisms of the end-effector. The wrench associated to the drilling operation is the one used for Fig. 6, which thus corresponds to the nominal hole operation task ($y = 0$ mm). We will consider a first scenario, referred as the *standard* scenario, where the orientation of the end-effector is fully constrained for each hole position (thus leading to 6 geometric constraints for the task) and where the position of the robot elbow (swivel angle) is set to a constant $\beta = 0°$. One may note that this first scenario is very likely to happen on real industrial applications, given that the default API of the robot currently doesn't allow easy exploitation its intrinsic redundancy. We will also consider a second scenario, referred as the *redundant* scenario, where the robot has the same 2-dimensional redundancy space as the one used for Fig. 6, for each hole position.

The simulations on Fig. 7 display, for 6 different designs of end-effectors, the variations of the FCI along the range of the hole plausible positions. In dashed lines are simulated the saturating intensities of the *standard* scenario. In thick lines are simulated the saturating intensities of the *redundant* scenario. Each simulated end-effector design corresponds to a different color on the graph of Fig. 7. It is worth noticing that the mechanical design of the end-effector has consequences on the

[3]That is to say a task constraining three DOFs for positioning and three others for orientating the TCP.

[4]Joint 7 solicitation does not change much over the entire redundancy space, and the joint is only very lightly burdened whatsoever.

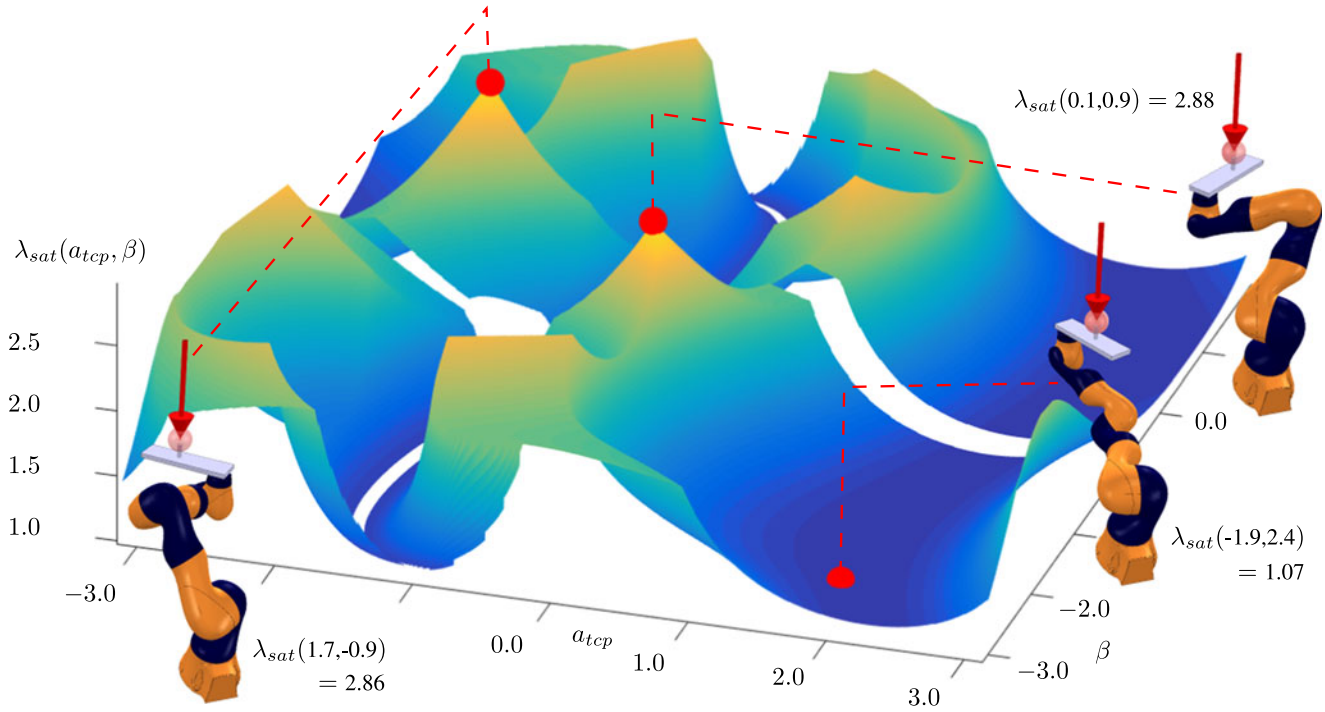

Fig. 6. Force saturating intensity of a KUKA LBR iiwa R820, mounted with a 5.0 kg end-effector, for a spatial force depicted by the red arrow (itself pointing at the TCP and along its z_{tcp} component) with translational component $\vec{\mathcal{R}}(EE \rightarrow ext) = [0\text{ (N)}, 0\text{ (N)}, -200\text{ (N)}]_{\mathcal{B}_{tcp}}$ and moment $\vec{\mathcal{M}}_{O_{tcp}}(EE \rightarrow ext) = [0\text{ (Nm)}, 0\text{ (Nm)}, 0\text{ (Nm)}]_{\mathcal{B}_{tcp}}$ (expressed at the TCP origin O_{tcp}, in its associated geometric basis $\mathcal{B}_{tcp}$). The 5-DOFs task is defined by the position : $[x, y, z] = [0.580\text{ (m)}, 0\text{ (m)}, 0.740\text{ (m)}]_{\mathcal{B}_0}$ and orientation (with XYZ-euler formalism) : $[\alpha_x, \beta_y, \gamma_z] = [0\text{ (rad)}, 0\text{ (rad)}, -0.8153 + a_{tcp}\text{ (rad)}]_{\mathcal{B}_0}$. The FCI value in redundancy space zones which are out of joint movement limits or otherwise unreachable don't appear on the figure (blank gaps).

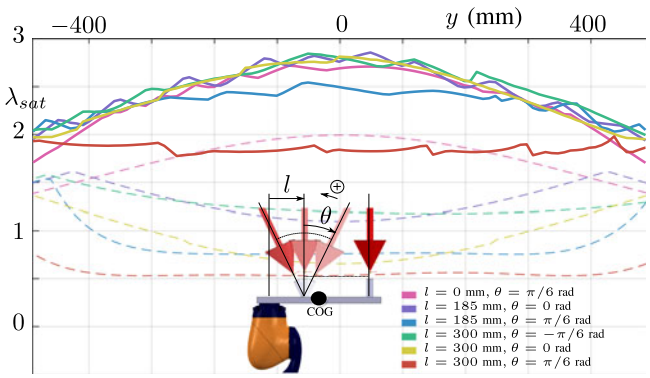

Fig. 7. Evolutions of λ_{sat} along the holes span for six different end-effector designs in the *standard* (dashed lines) and *redundant* (thick lines) scenarios accompanied by an illustration of the end-effector design DOFs.

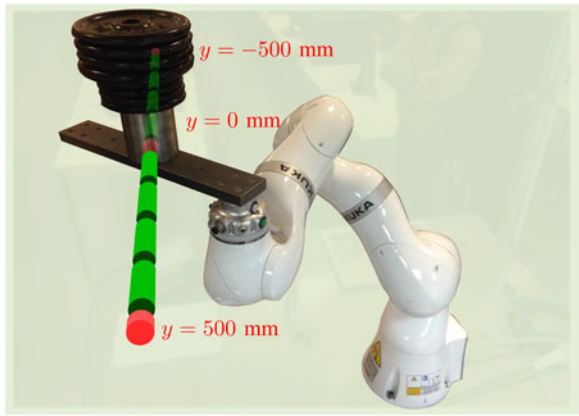

Fig. 8. Use case experimentation and illustration of the holes span. KUKA LBR iiwa easily withstanding 5 kg end-effector and 22 kg load.

manipulator force capacity that one would expect in the *standard* scenario (namely that the robot is getting weaker with regard to the wrench as l and θ increase), but that this behaviour becomes less obvious when full exploitation of redundancy is performed. Redundancy helps balancing torque solicitations on joints and sometimes gives astonishing results. Fig. 8 shows a practical test of this use case, for a 5 kg end-effector subject to a 22 kg payload, for $y = 0$ mm. The configuration used for this test is the same as the one displayed in the bottom left of Fig. 6, and proved to be uncharacteristically strong for this relatively low payload robot.

On the practical aspect of computations, the non convexity, non-smoothness and sometimes non-continuity of λ_{sat} function, which comes from taking the minimum of the (non-convex) saturating intensities,[5] from the non-reachability of some redundancy space positions and from joint limits, makes it a challenging problem for traditional optimisation approaches taking λ_{sat} as cost (or constraint) function, without guarantee of finding a

[5]For examples of non-smooth and non-convex saturating intensities, see Fig. 4.

global maximum. Local maxima would also be difficult to find for traditional optimisation techniques because they often lie on, or close to the intersections of different saturating intensities, i.e., areas where λ_{sat} function is not differentiable.

Low dimensional problems like the ones shown in this letter can be fully and efficiently solved by sampling the redundancy space of the manipulator and computing λ_{sat} for each sample. The sampling approach allows for a very thorough understanding of the possibilities redundancy offers. For higher dimensional problems (i.e., problems where the redundancy space has many degrees of freedom), it may be advisable to use optimisation techniques such as genetic algorithms, which are more suited to these kinds of functions than algorithms traditionally used in constrained non-linear optimisation (interior point, SQP, active set, trust region reflective, etc...) although they don't guarantee the repeatability of the result. Their use was experimented with success on 1-, 2- and 4-DOFs redundancy space, with good results (the local extrema shown on Fig. 6 are results of this genetic algorithm approach).

V. Conclusion

A real-valued index measuring the capacity extent of a serial manipulator, set in a given configuration, to produce a specific spatial force was described in this letter. A framework, based on a parameterisation of the self-motion of redundant manipulators, was then presented to help explore their redundancy space in search for strong values of the force capacity index.

Unlike polytopes, manipulability ellipsoids and DCE-linked tools, which focus on the overall force (and other physical quantities) capabilities in one given configuration, this method focuses on one particular force capacity over all the possible configurations offered by kinematic redundancy. The authors find this tool suitable for direct use, with the purpose of simplifying redundancy resolution and exploitation.

The relevance of the proposed approach was illustrated with a practical use case involving a discrete path planning and mechanical design problem. The use case demonstrated the advantage of exploiting the available redundancies of this system while demonstrating the simplicity of use of the FCI. The presented index was shown to have a strong dependency on the configuration used by the manipulator, which demonstrates its relevance for redundant robotic operations involving interactions.

Quite remarkably, KUKA LBR iiwa 14 R820 is shown to have force capabilities which extended well beyond what the worst-case-14 kg-equivalent-weight announced by the manufacturer could suggest (on the simulation of Fig. 6, more than 570 N can be withstood at the TCP).

Although force production may be extended well beyond what one could expect from a robot such as the LBR iiwa, it may be important, for industrial operations, to maintain a level of accuracy by limiting gear elastic deformations. An other index, developed in [17], proposes to assess the Cartesian rigidity along the direction of an interaction force over the redundancy space of a manipulator. This criteria, and maybe an other that measures translational and rotational displacements of the TCP could be combined with the one described in the letter to assess and improve the overall performances of redundant manipulators.

References

[1] T. Yoshikawa, "Manipulability of robotic mechanisms," *The Int. J. Robot. Res.*, vol. 4, no. 2, pp. 3–9, 1985.

[2] P. Chiacchio, Y. Bouffard-Vercelli, and F. Pierrot, "Force polytope and force ellipsoid for redundant manipulators," *J. Field Robot.*, vol. 14, no. 8, pp. 613–620, 1997.

[3] T. Kokkinis and B. Paden, "Kinetostatic performance limits of cooperating robot manipulators using force-velocity polytopes," in *Proc. ASME Winter Annu. Meet.*, 1989, pp. 151–155.

[4] A. Bowling and O. Khatib, "The dynamic capability equations: A new tool for analyzing robotic manipulator performance," *IEEE Trans. Robot.*, vol. 21, no. 1, pp. 115–123, Feb. 2005.

[5] B. Siciliano and O. Khatib, *Springer Handbook of Robotics*. New York, NY, USA: Springer, 2016.

[6] B. Siciliano, L. Sciavicco, L. Villani, and G. Oriolo, *Robotics: Modelling, Planning and Control*. New York, NY, USA: Springer, 2010.

[7] T. Yoshikawa, "Dynamic manipulability of robot manipulators," in *Proc. IEEE Int. Conf. Robot. Autom.*, 1985, vol. 2, pp. 1033–1038.

[8] P. Chiacchio, S. Chiaverini, L. Sciavicco, and B. Siciliano, "Influence of gravity on the manipulability ellipsoid for robot arms," *J. Dyn. Syst., Meas., Control*, vol. 114, no. 4, pp. 723–727, 1992.

[9] P. Chiacchio and M. Concilio, "The dynamic manipulability ellipsoid for redundant manipulators," in *Proc. IEEE Int. Conf. Robot. Autom.,* 1998, vol. 1, pp. 95–100.

[10] P. Chiacchio, "A new dynamic manipulability ellipsoid for redundant manipulators," *Robotica*, vol. 18, no. 04, pp. 381–387, 2000.

[11] J. Lee, "A study on the manipulability measures for robot manipulators," in *Proc. IEEE /RSJ Int. Conf. Intell. Robots Syst.,* 1997, vol. 3, pp. 1458–1465.

[12] O. Khatib and J. F. L. Maitre, "Dynamic control of manipulators operating in a complex environment," in *Proc. 3rd CISM-IFToMM Symp. Theory Practice Robots Manipulators*, Udine, Italy, Sep. 1978, pp. 267–282.

[13] D. Zhou, L. Ji, Q. Zhang, and X. Wei, "Practical analytical inverse kinematic approach for 7-dof space manipulators with joint and attitude limits," *Intell. Service Robot.*, vol. 8, no. 4, pp. 215–224, 2015.

[14] Y. Wang, "Closed-form inverse kinematic solution for anthropomorphic motion in redundant robot arms," Ph.D. dissertation, Arizona State Univ., Tempe, AZ, USA, 2013.

[15] D. Tolani, A. Goswami, and N. I. Badler, "Real-time inverse kinematics techniques for anthropomorphic limbs," *Graph. Models*, vol. 62, no. 5, pp. 353–388, 2000.

[16] P. Dahm and F. Joublin, "Closed form solution for the inverse kinematics of a redundant robot arm," Inst. Neuroinf, Ruhr Univ. Bochum, Germany, Tech. Rep. IR-INI 97–08, 1997.

[17] D. Busson, R. Béarée, and A. Olabi, "Task-oriented rigidity optimization for 7-DOFs redundant manipulators," Toulouse, France,in *Proc.World Congr. Int. Fed. Autom. Control*, 2017, pp. 14588–14593.